CD34 Expression by Hair Follicle Stem Cells Is Required for Skin Tumor Development in Mice

Carol S. Trempus,[1] Rebecca J. Morris,[6] Matthew Ehinger,[7] Amy Elmore,[7] Carl D. Bortner,[2] Mayumi Ito,[8] George Cotsarelis,[8] Joanne G.W. Nijhof,[9] John Peckham,[3] Norris Flagler,[3] Grace Kissling,[4] Margaret M. Humble,[1] Leon C. King,[5] Linda D. Adams,[5] Dhimant Desai,[10] Shantu Amin,[10] and Raymond W. Tennant[1]

[1]Cancer Biology Group, Laboratory of Molecular Toxicology, [2]Laboratory of Signal Transduction, [3]Laboratory of Experimental Pathology, and [4]Biostatistics Branch, National Institute of Environmental Health Sciences; [5]National Health and Environmental Effects Research Laboratory, United States Environmental Protection Agency, Research Triangle Park, North Carolina; [6]Department of Dermatology, Columbia University Medical Center, New York, New York; [7]Integrated Laboratory Systems, Inc., Durham, North Carolina; [8]Department of Dermatology, University of Pennsylvania, School of Medicine, Philadelphia, Pennsylvania; [9]Department of Dermatology, Leiden University Medical Center, Leiden, the Netherlands; and [10]Department of Pharmacology, Pennsylvania State Milton S. Hershey Medical Center, Hershey, Pennsylvania

Abstract

The cell surface marker CD34 marks mouse hair follicle bulge cells, which have attributes of stem cells, including quiescence and multipotency. Using a CD34 knockout (KO) mouse, we tested the hypothesis that CD34 may participate in tumor development in mice because hair follicle stem cells are thought to be a major target of carcinogens in the two-stage model of mouse skin carcinogenesis. Following initiation with 200 nmol 7,12-dimethylbenz(*a*)anthracene (DMBA), mice were promoted with 12-*O*-tetradecanoylphorbol-13-acetate (TPA) for 20 weeks. Under these conditions, CD34KO mice failed to develop papillomas. Increasing the initiating dose of DMBA to 400 nmol resulted in tumor development in the CD34KO mice, albeit with an increased latency and lower tumor yield compared with the wild-type (WT) strain. DNA adduct analysis of keratinocytes from DMBA-initiated CD34KO mice revealed that DMBA was metabolically activated into carcinogenic diol epoxides at both 200 and 400 nmol. Chronic exposure to TPA revealed that CD34KO skin developed and sustained epidermal hyperplasia. However, CD34KO hair follicles typically remained in telogen rather than transitioning into anagen growth, confirmed by retention of bromodeoxyuridine-labeled bulge stem cells within the hair follicle. Unique localization of the hair follicle progenitor cell marker MTS24 was found in interfollicular basal cells in TPA-treated WT mice, whereas staining remained restricted to the hair follicles of CD34KO mice, suggesting that progenitor cells migrate into epidermis differently between strains. These data show that CD34 is required for TPA-induced hair follicle stem cell activation and tumor formation in mice. [Cancer Res 2007;67(9):4173–81]

Introduction

The skin is a complex organ, composed in part of a stratified epidermis that undergoes continual renewal. The regenerative capacity of the epidermis is conferred by stem and progenitor cells residing in the hair follicle and interfollicular epidermis (1–3). It is widely recognized that a population of multipotent stem cells is localized to the bulge region of the hair follicle, which is a distinct "niche" that is relatively protected from external damage and participates in normal follicular growth/rest cycling (1, 4). However, recent evidence has shown that, although epidermal stem cells in the bulge region do not actively participate in epidermal homeostasis (5–7), they do contribute to wound repair (6).

There has been considerable discussion of the role of hair follicle stem cells in skin carcinogenesis (8, 9). The two-stage model of mouse skin carcinogenesis is based on a large body of data in mice exposed to a specific initiation-promotion regimen, which involves treatment of the skin with a subtumorigenic dose of a carcinogen followed by exposure to a tumor promoter, inducing chronic regenerative hyperplasia. Mutated cells then undergo expansion, forming benign papillomas and eventually cancerous lesions (10, 11). The two-stage model provides insights into the nature of the cell populations at risk for tumor development in addition to lending insight into the mutational events that contribute to this process. Recent evidence has shown that papillomas can arise from initiated cells harbored within two distinct compartments within the skin: the interfollicular epidermis and within the hair follicle (12). Because initiated skin retains the ability to form papillomas, even with long intervals between carcinogen exposure and tumor promotion, it is believed that carcinogen target cells are composed at least in part of epidermal stem cells in the hair follicle bulge region, which are preserved over the life of the animal through many hair follicle generations. Thus, it has been proposed that, in the two-stage mouse model of skin carcinogenesis, hair follicle epidermal stem cells are carcinogen target cells that give rise to a population of latent neoplastic cells that contribute, along with target cells within the interfollicular epidermis, to tumor development (8, 9).

Characterization and experimental manipulation of mouse hair follicle stem cells has become possible in recent years due to the discovery of cell surface markers capable of enriching bulge-derived stem cells with fluorescence-activated cell sorting (FACS; refs. 13–15) and the generation of transgenic mouse models (4, 16, 17). Recently, it has been shown that the cell surface glycoprotein CD34 is uniquely

Note: The research described in this manuscript has been reviewed by the National Health and Environmental Effects Research Laboratory, U.S. Environmental Protection Agency, and approved for publication. Approval does not signify that the contents necessarily reflect the views and policies of the Agency nor does mention of trade names or commercial products constitute endorsement or recommendation for use.

Requests for reprints: Carol S. Trempus, National Institute of Environmental Health Sciences, 111 TW Alexander Drive, Mail Drop F1-05, Research Triangle Park, NC 27709. Phone: 919-541-0240; Fax: 919-541-1460; E-mail: trempus@niehs.nih.gov.

doi:10.1158/0008-5472.CAN-06-3128

expressed on mouse hair follicle bulge keratinocytes (15), and the cell surface properties of CD34 have facilitated isolation of living keratinocytes with stem cell characteristics from mouse hair follicles (15, 18). In addition to keratinocytes, CD34 is expressed on mouse hematopoietic stem and progenitor cells (19) as well as on more differentiated cell types, including mast (20) and endothelial cells (21). Poblet et al. (22) first reported that CD34 is expressed in human hair follicles, specifically in the outer root sheath cells of anagen follicles, although recent evidence shows that CD34 is not expressed specifically in the bulge region of human hair follicles (23, 24). However, CD34-expressing outer root sheath cells in human hair follicles do not coexpress Ki67, so this is likely a quiescent population of cells.[11]

Recent evidence suggests that the function of CD34 is dependent on cellular context [e.g., CD34 acts as an adhesion molecule in specialized blood vessels (reviewed in ref. 25) but as an antiadhesion molecule in mast cells (26)], and its activity is potentially regulated by cytosolic binding proteins (27). In the mouse, CD34 specifically localizes to hair follicle stem cells, which are thought to be carcinogen targets and the cells of origin for skin tumors in mice and humans. We therefore investigated the role of CD34 in cutaneous papilloma formation using a CD34 knockout (KO) line developed by Suzuki et al. (28). Tumor development was abrogated or significantly delayed depending on the initiating dose of 7,12-dimethylbenz(*a*)anthracene (DMBA), which was shown to be metabolically activated into carcinogenic DNA adducts. We present evidence that hair follicle bulge cells lacking CD34 expression have a delayed response to 12-*O*-tetradecanoylphorbol-13-acetate (TPA)-induced proliferation, resulting in delayed anagen onset, indicating that CD34 plays a major role in hair follicle bulge stem cell activation. In addition, we found that basal cells within the interfollicular epidermis of CD34KO mice lack TPA-induced reactivity with the hair follicle progenitor cell surface marker MTS24 (29), which, shown here for the first time, is abundantly expressed in the interfollicular epidermis of TPA-treated wild-type (WT) mice. These studies show that CD34 is critical for epithelial carcinogenesis in mouse skin, with effects in stem cell activation and migration of initiated cells out of the hair follicle.

Materials and Methods

Animals. To generate colonies of mice for experimental procedures, breeding pairs of CD34KO mice were obtained from Dr. T.W. Mak (University of Toronto, Toronto, Ontario, Canada; ref. 28) and maintained in the animal facility of Integrated Laboratory Systems, Inc. (Durham, NC) in accordance with institutional guidelines for the care and use of laboratory animals. B6.129F1 control animals were purchased from The Jackson Laboratory, and C57BL/6 WT control animals were purchased from Charles River Laboratories, Inc.

Chemicals. DMBA and TPA were obtained from Sigma-Aldrich and prepared in acetone (Fisher Scientific) for animal studies. Bromodeoxyuridine (BrdUrd; Sigma-Aldrich) was prepared in saline to deliver 50 μg/dose [label-retaining cell (LRC) experiment]. The ± *anti*-7,12-DMBA-3,4-dihydro-1,2-epoxide (*anti*-DMBADE) and ± *syn*-7,12-DMBA-3,4-dihydro-1,2-epoxide (*syn*-DMBADE) were synthesized by previously reported methods (30, 31) and were >98% pure.

Immunohistochemical characterization of CD34KO and WT skin. Whole skin was either fixed overnight in 10% neutral buffered formalin (NBF) or frozen in OCT compound (Tissue-Tek; American Master*Tech Scientific). Antibodies used for immunohistochemistry included rat anti-mouse CD34 (BD PharMingen) and mouse anti-human BrdUrd (BD PharMingen). Specifics for CD34 immunostaining are described previously (15). Protocol details for BrdUrd staining in paraffin sections can be found at the National Institute of Environmental Health Sciences Laboratory of Experimental Pathology (Special Techniques Group) Web site.[12] MTS24 immunostaining was done essentially as described elsewhere (29).

Keratinocyte harvest and flow cytometry. Keratinocytes were harvested from 7-week-old WT and CD34KO mice as described previously (32). Single-cell suspensions were stained with antibodies to CD34 and α_6 integrin (both from BD PharMingen) as described elsewhere (15) for FACS analysis. Cells were examined on a FACSVantage SE flow cytometer equipped with digital electronics (Becton Dickinson), with propidium iodide added just before examination. All samples were excited at 488 nm, and FITC, propidium iodide, and cychrome were detected at 530, 575, and 660, respectively. Ten thousand cells were examined per sample and analyzed using BD FACSDiva software.

Skin tumor experiments. Seven-week-old CD34KO and WT male and female mice were initiated with 200 (experiments 1 and 2) or 400 nmol (experiment 3) DMBA in 200 μL acetone. One week later, mice were dosed topically thrice weekly with either 4 μg TPA in 200 μL acetone (experiments 1 and 2), 5 μg TPA in 200 μL acetone (experiment 3), or acetone alone (200 μL; all experiments) for 20 weeks. Experiments 1 and 2 were conducted using both male and female CD34KO and B6.129 mice (experiment 1 included 10 males and 10 females, and experiment 2 included 10 males and 5 females). Small numbers of mice were placed into additional control groups (total of five mice per group, using both male and female), including DMBA (once) + acetone (thrice weekly), acetone (once) + TPA (thrice weekly), and acetone (once) + acetone (thrice weekly). For experiment 3, male and female CD34KO and C57BL/6 mice were used (seven males and six females for both strains). Papilloma development was tracked weekly for 20 weeks in experiments 1 and 3 and for 25 weeks in experiment 2. A papilloma was counted if ≥1 mm in size.

Analysis of DNA adduct formation by ^{32}P-postlabeling. Mice were dosed with either 200 or 400 nmol DMBA, and keratinocytes were harvested (15, 32) 24 h after initiation. Calf thymus DNA adducts were prepared with stock *anti*-DMBADE and *syn*-DMBADE and extracted as described elsewhere (33). The procedures used in the reactions of *anti*-DMBADE and *syn*-DMBADE with 3′-dGMP and 3′-dAMP were a modification of the techniques described by Lau and Baird (34). For ^{32}P-postlabeling, analysis of genomic DNA isolated from DMBA-initiated keratinocytes was conducted as described elsewhere (35–37). Separation of ^{32}P-labeled nucleoside-3′,5′-bisphosphate adducts was carried out on a Hewlett-Packard Series 1100 HPLC System (Hewlett-Packard Co.) using a 5 μm, 4.6 mm × 250 mm Zorbax phenyl-modified column (MAC-MOD Analytical, Inc.). Radiolabeled nucleotides were detected by scintillation counting, and retention times of ^{32}P-postlabeled DNA adducts were expressed as relative retention time (RRT), calculated by dividing the retention time of the ^{32}P-postlabeled DNA adducts by the retention time of the internal standard (*cis*-9,10-dihydroxy-9,10-dihydrophenanthrene; a gift from Dr. David H. Phillips, Haddow Laboratories, The Institute of Cancer Research, Sutton, Surrey, United Kingdom). The reproducibility of the RRT is ±0.03.

Assessment of the epidermal response of CD34KO and WT mice to chronic TPA exposure. The skin of seven-week-old CD34KO and WT male and female mice was dosed with four applications of either 5 or 10 μg TPA in 200 μL acetone, administered twice weekly over 2 weeks (4 × 5 μg and 4 × 10 μg, respectively), and tissues were collected 24 or 48 h after the last dose following a 1-h exposure to BrdUrd (i.p. at 50 mg/kg). To ensure that animals were in the resting (telogen) stage of the hair follicle cycle at start of treatment, mice were shaved 2 days before dosing. Animals showing hair regrowth at the time of first dosing were not used in these experiments. A single piece of skin was taken from the site of application, fixed in 10% NBF, and prepared for histologic examination as well as immunostaining. For

[11] C.S. Trempus and G. Cotsarelis, unpublished observations.

[12] http://dir.niehs.nih.gov/dirlep/immuno/protocols.htm

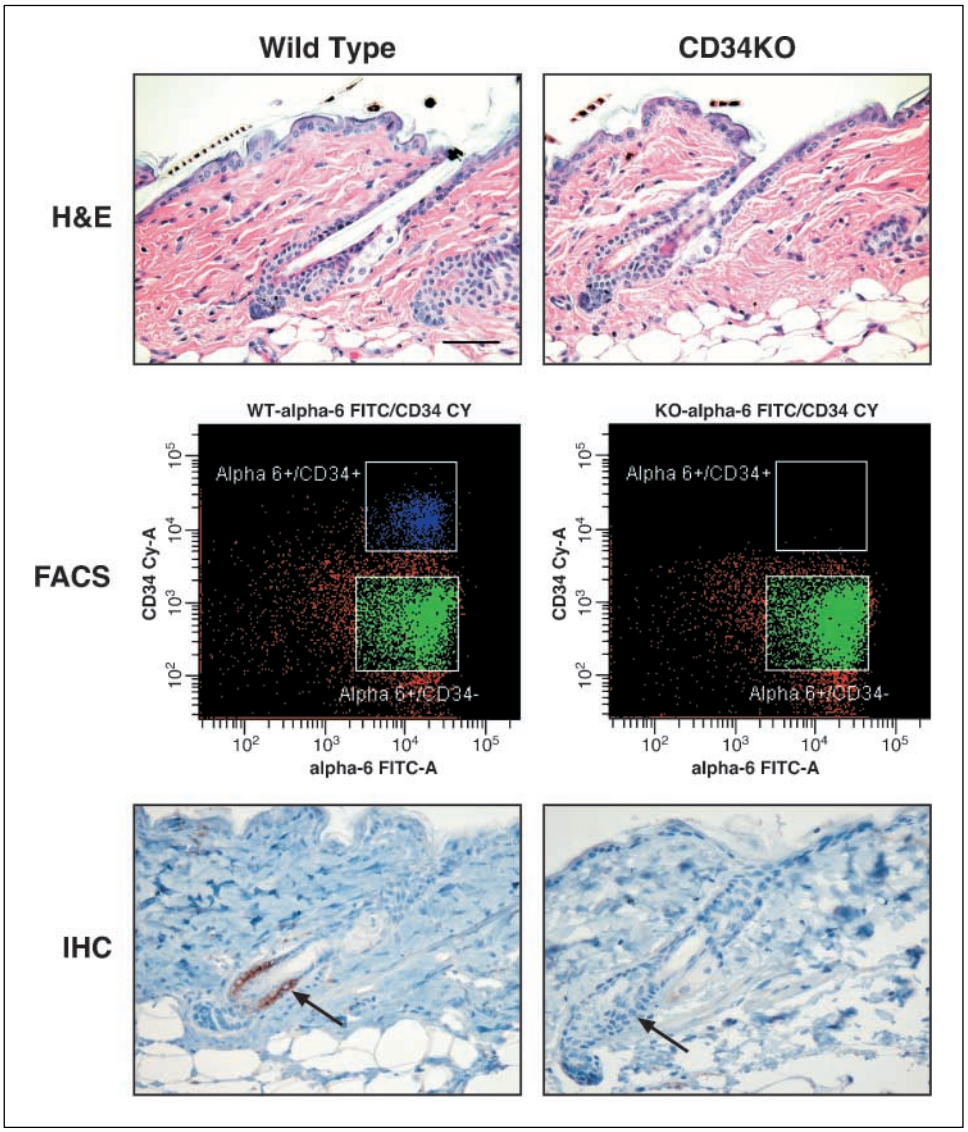

Figure 1. CD34KO mouse skin lacks CD34 expression and appears normal histologically. *Top,* skin from 7-wk-old WT and CD34KO mice was fixed in 10% formalin and stained with H&E; *middle,* single-cell suspensions of keratinocytes were stained with antibodies to α_6 integrin and CD34 and analyzed by FACS; *bottom,* formalin-fixed sections were stained with a rat anti-mouse CD34 antibody. *Bar*, 50 μm.

photomicrograph preparation, slides were scanned at 200× using the Aperio ScanScope T2 Scanner (Aperio Technologies, Inc.) to capture high-resolution, seamless digital images. After scanning, slides were viewed using Aperio ImageScope v. 6.25.117 (Aperio Technologies) to capture images. Photomicrographs were also prepared using an Olympus BX51 microscope (Opelco) combined with a Sony iCY-SHOT DXC-S500 digital camera (Sony Corp.).

LRC formation and response to TPA. Three-day-old CD34KO and WT pups were injected twice daily for 3 days with BrdUrd at 50 μg/dose, for a cumulative daily dose of 100 μg. Skin was collected 7 weeks after the last dose to assess LRC formation and localization under steady-state conditions. To assess bulge cell response to TPA exposure, 7-week-old mice injected with BrdUrd as pups were treated topically with TPA (4 × 5 μg or 4 × 10 μg), with skin collected 24 and 48 h after the last dose. LRC localization was assessed using light microscopic examination of BrdUrd-stained tissues.

Statistics. Percentages of tumor-bearing animals were compared between CD34KO and WT mice using Fisher's exact test at each week.

Results

Characterization of CD34KO Mouse Skin

The skin of CD34KO mice was compared with that of WT mice to (*a*) determine if a skin phenotype was apparent in untreated CD34KO epidermis and (*b*) confirm that CD34 expression was lost in hair follicle keratinocytes. CD34KO mice were originally on a C57BL/6.129 background, with backcrosses to C57BL/6 mice made by the developing laboratory. In the current experiments, B6.129 mice as well as C57BL/6 mice were used as the WT control to address the unknown amount of 129 retained in the CD34KO genetic background, which is of particular concern because the 129 background confers sensitivity to tumor induction protocols (38) and residual 129 can still affect phenotype even after as many as 10 backcrosses to C57BL/6 (39). The WT strain shown for most experimentation described herein is from comparisons to the B6.129 background unless otherwise noted. H&E-stained sections from 7-week-old CD34KO mice showed normal morphology, spacing, and orientation of hair follicles and normal epidermal thickness (Fig. 1, *top*). As expected, no CD34 expression was detected in single-cell suspensions of keratinocytes or in formalin-fixed sections of CD34KO skin (Fig. 1, *FACS* and *IHC*, respectively). Expression of keratin 15 (40), S100A4, and S100A6 (data not shown; ref. 41) was detected in the hair follicles of both strains, indicating normal expression and localization of other bulge markers. These data confirm normal

morphology of the hair follicle bulge region despite the absence of CD34 expression in CD34KO mice.

Tumor Development in DMBA-Initiated, TPA-Promoted CD34KO Mice

The combination of CD34 localization to a hair follicle epidermal stem cell population in conjunction with these cells as probable targets of carcinogens led us to hypothesize that CD34 may play a role in skin tumor formation in mice. To test this hypothesis, 7-week-old CD34KO (28) and WT B6.129 mice were first initiated with 200 nmol DMBA and then promoted with TPA, and tumor development was followed for at least 20 weeks in two independent studies. Under these conditions, no skin papillomas were detected on DMBA-initiated/TPA-promoted male or female CD34KO mice (Fig. 2*A* and *B*). In contrast, both male and female WT mice developed papillomas following initiation and promotion. Because male WT mice had a higher tumor frequency than female WT mice, tumor multiplicity (average number of tumors per mouse; Fig. 2*A*) and tumor incidence (percentage tumor-bearing mice; Fig. 2*B*) are shown for male mice only. By week 12 in experiment 1, significantly more WT mice had tumors ($P < 0.05$) than did CD34KO, and this occurred by week 11 in experiment 2 ($P < 0.02$). By the end of each study, the statistical significance had strengthened ($P < 0.0001$ and 0.0004 for experiments 1 and 2, respectively) as tumor multiplicity increased in WT mice, whereas CD34KO remained tumor-free.

An additional tumor experiment was conducted with CD34KO using C57BL/6 mice as the WT strain, and in this case, the initiating dose of DMBA was increased to 400 nmol, and the promoting dose of TPA was increased from 4 to 5 μg per application. The purpose here was to compare the CD34KO mouse to an alternate WT strain and to test the effect of a more stringent initiation-promotion regimen on tumor development, given the predominant C57BL/6 background of the KO mice. Although both males and females were used in this experiment, data for males only are shown, as females were not uniformly in telogen at initiation. As shown in Fig. 2*C* and *D*, male CD34KO mice developed papillomas late in the study, starting at week 15 of promotion, compared with week 8 for the WT mice. In addition, the overall tumor numbers were lower in the CD34KO mice by week 20 (average of 0.4 ± 0.3 papillomas per mouse for the CD34KO males compared with 4.6 ± 1.6 for WT; $P < 0.03$). Female CD34KO mice also developed a low incidence of tumors (data not shown), although one female developed a single papilloma at week 8 of promotion and went on to develop four papillomas by end of study. Therefore, increasing the dose of DMBA resulted in papilloma development with a significantly increased latency and reduction in overall tumor numbers, confirming an important role for CD34 in tumor development.

The results of the tumor experiments described above suggest a critical role for CD34 in either the initiation or promotion stages, although the ability to form at least some tumors implicates a stronger role in promotion. However, because of the lack of a tumor response at the 200 nmol dose of DMBA and the attenuated response at 400 nmol DMBA, we were interested in assessing the

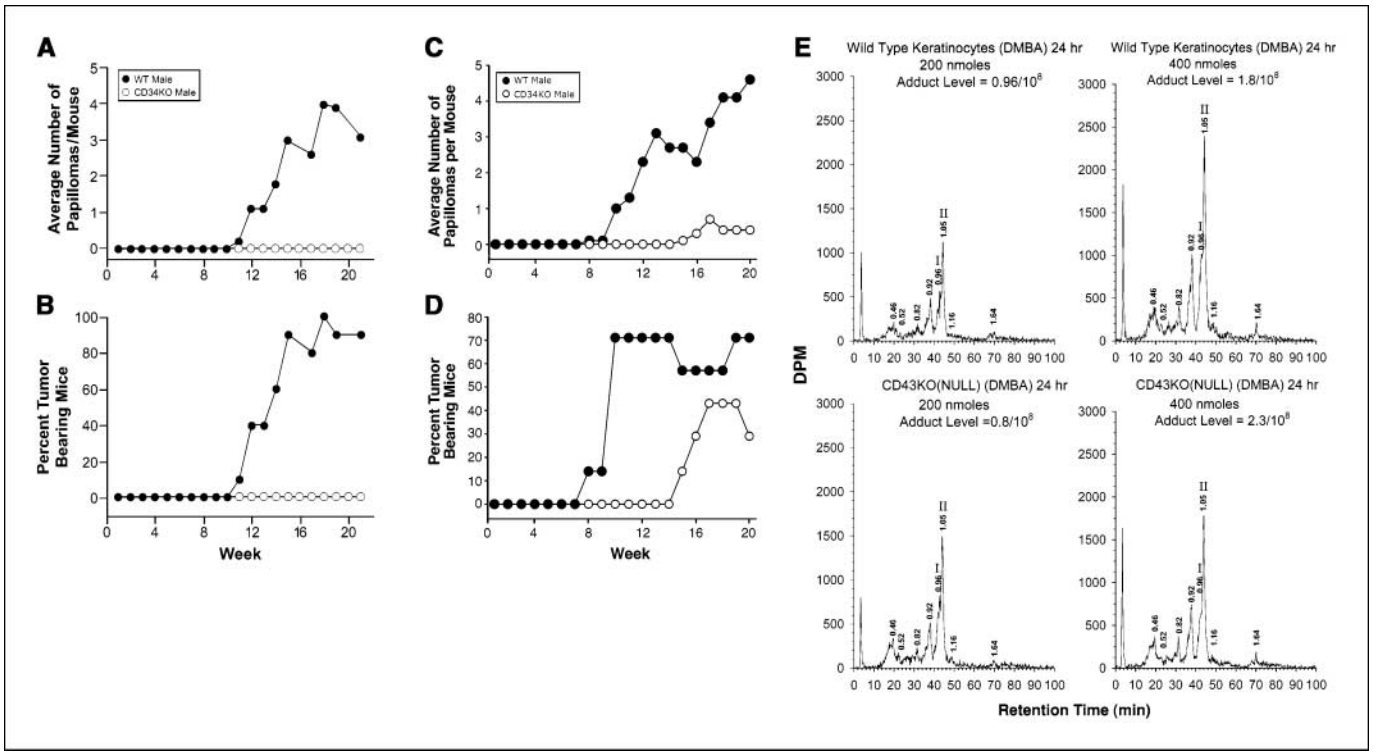

Figure 2. Papilloma development in DMBA-initiated, TPA-promoted CD34KO mice. Seven-week-old CD34KO and WT mice were first initiated with subtumorigenic doses of DMBA and then promoted for 20 weeks with three applications per week of TPA in the standard two-stage mouse skin carcinogenesis regimen. Papillomas were counted weekly. *A* and *B,* mice were initiated with 200 nmol DMBA and then promoted thrice weekly with 4 μg TPA for 20 wks. *A,* average number of tumors per mouse. *B,* incidence of papillomas. *C* and *D,* CD34KO and WT mice were initiated with 400 nmol DMBA and then promoted thrice weekly with 5 μg TPA for 20 wks. *C,* average number of tumors per mouse. *D,* incidence of papillomas. *E,* mice were initiated with either 200 or 400 nmol DMBA, and keratinocytes were harvested 20 h later for DNA isolation and ^{32}P-postlabeling identification of DMBADE DNA adducts. *Top,* DNA adducts for WT at 200 and 400 nmol; *bottom,* DNA adducts for CD34KO mice at 200 and 400 nmol. *Syn*-dAdo and *anti*-dAdo adducts are identified as *I* (retention time, 0.96 min) and *II* (retention time, 1.05 min), respectively.

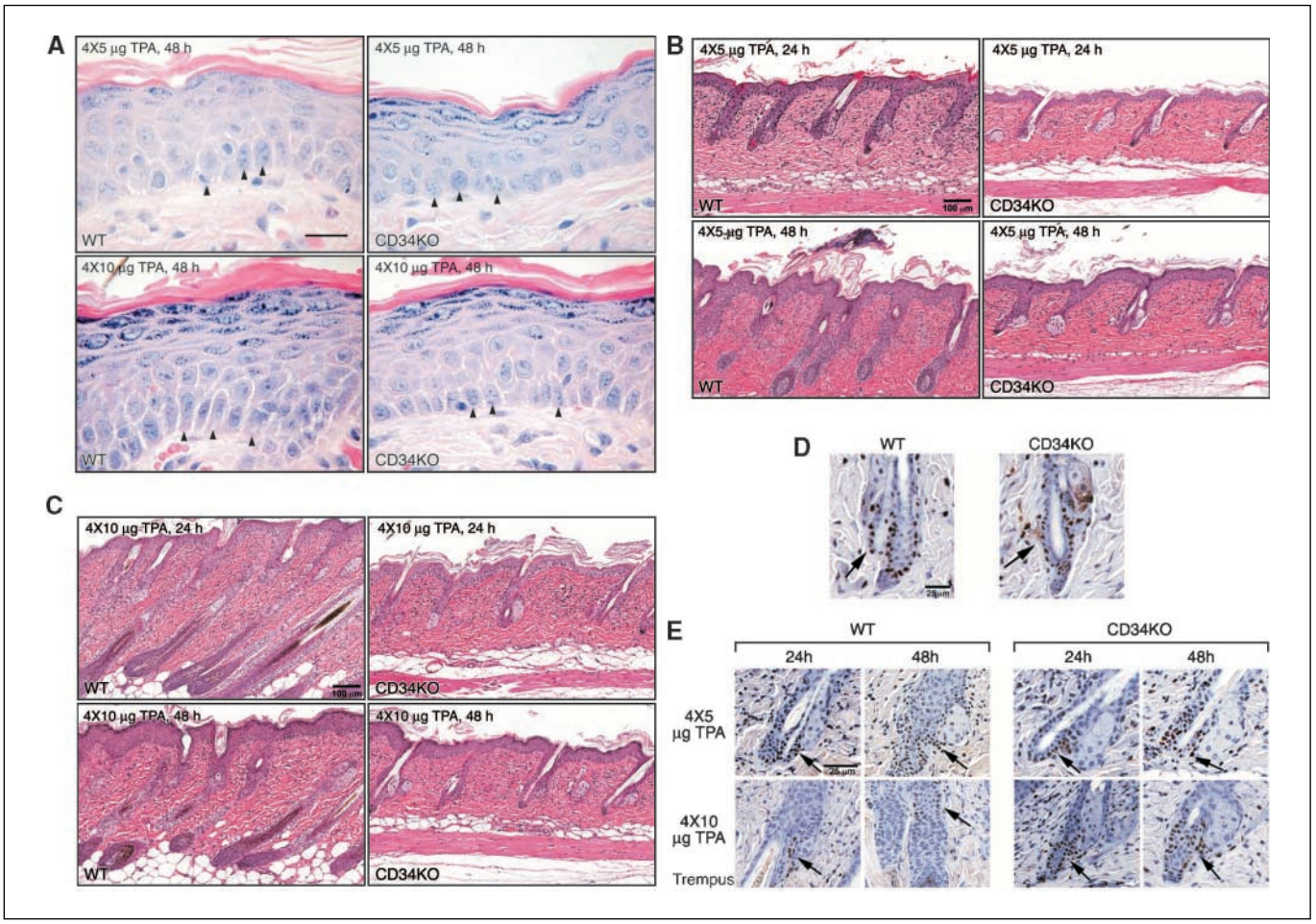

Figure 3. Response of CD34KO epidermis and hair follicles to short-term TPA exposure. To test the ability of CD34KO skin to develop epidermal hyperplasia, 7-wk-old WT and CD34KO mice were subjected to short-term TPA exposure. Mice were dosed twice weekly for 2 wks with either 5 or 10 μg of TPA, and tissues were collected at 24 and 48 h after the last dose. In addition, beginning at postnatal day 3, CD34KO and WT pups were injected with BrdUrd twice daily for 3 d to generate LRCs. Tissues were fixed in formalin, sectioned, and stained with anti-BrdUrd to identify the quiescent LRCs both under steady-state conditions and after TPA treatment. *A,* H&E-stained, high-magnification photomicrographs of the interfollicular epidermis in WT (*left*) and CD34KO (*right*) to both doses of TPA, 48 h only. Bar, 20 μm. *Arrowheads,* basal cells. Compare the simple cuboidal cells of the CD34KO mouse with the irregular layers of larger elongated basal cells of WT mice. *B* and *C,* photomicrographs of H&E-stained skin taken 24 and 48 h after the last dose of either 4 × 5 μg TPA or 4 × 10 μg TPA. Bar, 100 μm. In WT mice, previously resting hair follicles enter the growing stage in response to TPA treatment. In contrast, hair follicles in CD34KO mice remain in telogen, the resting phase of the hair cycle. *Left,* WT images; *right,* CD34KO images. Compare the small inactive hair follicles and thin epidermis of CD34KO mice with the large active growing hair follicles extending deep into the thick dermis of WT mice. *D,* LRC localization in WT and CD34KO hair follicles after a 7-wk chase. Bar, 25 μm. *E,* LRC response after TPA treatment. *Left,* WT; *right,* CD34KO. Bar, 25 μm. *Arrows,* bulge. Note in (*E*) the highly cellular, active hair follicles in WT mice.

ability of the CD34KO mice to metabolically activate DMBA. In order for a papilloma response to be elicited in DMBA-initiated tumorigenesis, DMBA must be metabolically activated by members of the P450 family into DMBADEs (10). DNA adducts form from these metabolites, particularly to the adenine residue in codon 61 in the c-Ha-*ras* proto-oncogene, ultimately forming a permanent mutation in *ras* (A to T transversion; ref. 10). In general, this is considered to be the causal event in the two-stage skin tumor model, as >90% of DMBA-induced papillomas carry this mutation (42).

CD34KO and WT C57BL/6 mice were dosed with either 200 or 400 nmol DMBA and keratinocytes were harvested 24 h after exposure, and then DNA adduct formation was assessed by ^{32}P-postlabeling analysis (Fig. 2*E*). Additionally, a group of CD34KO and WT B6.129 mice was initiated with 200 nmol DMBA for adduct analysis 24 h after exposure (data not shown). The primary carcinogenic DMBADEs *syn*-dAdenine and *anti*-dAdenine [dAdo; retention times of 0.96 min (I) and 1.05 min (II), respectively] were present in both strains at both doses at similar levels (Fig. 2*D*), although total adenine adduct levels were slightly lower in CD34KO mice at the 400 nmol dose of DMBA (Fig. 2*E*). However, these data showed that DMBA was metabolically activated by CD34KO keratinocytes at both doses of DMBA. Therefore, we conclude from this evidence as well as from the ability to form at least some tumors at the higher dose of DMBA that the defect in tumor development in the CD34KO mouse is not due to a lack of metabolic activation of DMBA and DNA adduct formation critical for papilloma development in the initiation stage.

Response of CD34KO Skin to Chronic TPA Exposure

Because our evidence ruled out a significant effect of CD34 on tumor development in the initiation phase in the two-stage model, we were interested in investigating factors that affect promotion. Tumors develop from initiated cells in the skin during promotion partially as a consequence of chronic epidermal hyperplasia (10). Therefore, we undertook experiments to study the epidermal and

hair follicle bulge stem cell response in CD34KO mice following chronic exposure to TPA.

Histologic evaluation of response to TPA. Both WT and CD34KO mice responded to TPA with moderate hyperplasia of the epidermis, although epidermal thickness was increased in WT skin at both dose levels (shown WT B6.129; Fig. 3*A–C*). Interestingly, the numbers of BrdUrd-positive cells in the interfollicular epidermis after pulse labeling for 1 h before euthanasia were similar between the two strains (data not shown). The organization of the keratin layer was similar between strains, with no differences either histologically or with immunostaining using keratin markers (data not shown). At both doses of TPA, basal cells of the interfollicular epidermis were small and uniformly cuboidal in the CD34KO skin (48-h time point shown for 4 × 5 μg and 4 × 10 μg TPA; Fig. 3*A, arrowheads*), whereas the basal layer in WT mice was characterized by increased numbers of basal cells, often having large elongated rectangular shapes characteristic of activated keratinocytes (48-h time point shown for 4 × 5 μg and 4 × 10 μg TPA; Fig. 3*A, arrowheads*). Although epidermal thickness was greater in WT B6.129 mice at both treatments and at both time points, epidermal thickness was similar between CD34KO and C57BL/6 mice after TPA treatment (data not shown), indicating that the difference in hyperplasia between CD34KO and B6.129 mice was possibly due to the C57BL/6 component of the KO strain background.

Because inflammation is a critical factor in skin tumor development in mice (10), and because CD34KO mice have been shown to have perturbations in mast cell recruitment (26) and eosinophil accumulation after allergen exposure in the lung (28), we carefully examined the dermal compartment for differences between strains in inflammatory cell composition after TPA exposure. Inflammatory cell composition was similar between the CD34KO mouse and the two WT strains, consisting of small numbers of eosinophils and some neutrophils, although inflammation was more severe in the higher dose of TPA. Mast cell numbers were similar between strains as well, as indicated by staining with toluidine blue (data not shown). These data indicate that a defect in inflammation is not an underlying factor in the skin tumor phenotype in CD34KO mice.

Delay in hair follicle cycling in CD34KO mice. A striking feature of TPA-exposed CD34KO skin was found in the hair follicle response. TPA exposure results in the activation of bulge stem cells, leading to entry of the hair follicle into anagen growth (1, 43, 44). Before TPA treatment, all mice were clipped to ensure that the skin was in the telogen or resting stage, based on lack of hair growth 24 to 48 h after clipping. After treatment, as seen in Fig. 3*B* and *C*

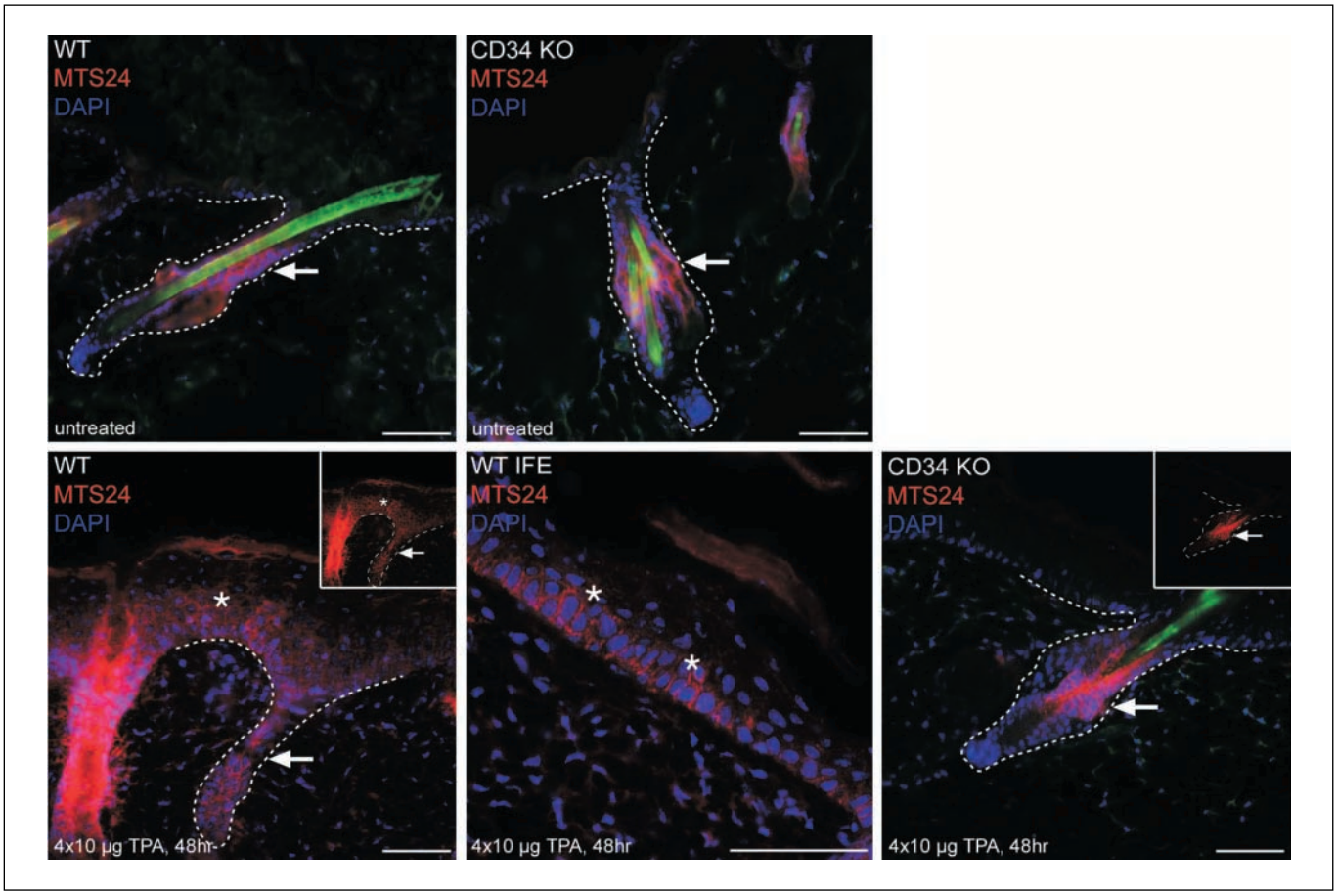

Figure 4. Localization of the hair follicle progenitor cell marker MTS24 in WT and CD34KO skin. To determine if lack of CD34 expression in hair follicles affected the localization of the hair follicle progenitor marker, untreated and TPA-treated CD34KO and WT skin was subjected to immunostaining with a mouse-specific MTS24 antibody. *Top,* localization to the midportion of telogen hair follicles (*arrows*) in untreated WT and CD34KO skin (7 wks of age); *bottom,* staining in anagen hair follicles (*arrow*) 48 h after the last of four applications of TPA (10 μg/dose). Note staining in the interfollicular epidermis extending into the suprabasal layers (*). *Bottom middle,* higher-magnification view of MTS24 labeling in basal cells of the interfollicular epidermis in WT skin after TPA (*); *bottom right,* MTS24 staining remains restricted to hair follicles in CD34KO (*arrows*) after TPA treatment. *Insets,* MTS24 staining (*red*) without 4′,6-diamidino-2-phenylindole (*DAPI*; *blue*). *Bar*, 50 μm.

(4 × 5 μg TPA and 4 × 10 μg TPA, respectively), hair follicles were typically in anagen in WT skin, with large, heavily pigmented, and basophilic hair bulbs extending deep into the dermis. In contrast, hair follicles in TPA-treated CD34KO remained in telogen or early anagen regardless of dose or time after the last dose. Supplemental studies using C57BL/6 as control animals confirmed that the hair follicle phenotype was unique to the CD34KO (data not shown). These data indicate that hair follicle bulge cells exhibited delayed activation in response to proliferative signals from the hyperplastic epidermis or from inflammatory cells in the dermis in CD34KO mice.

Proliferative response of CD34KO hair follicle bulge cells to TPA. To study directly the effect of TPA exposure on hair follicle bulge keratinocytes, we generated LRCs, a widely accepted *in vivo* marker of slowly cycling epidermal stem cells (1, 45). Three-day-old CD34KO and WT pups were injected with BrdUrd twice daily until postnatal day 6 and then maintained without treatment for 7 weeks. Control animals were euthanized at the end of 7 weeks. Experimental animals were dosed with TPA (4 × 5 μg or 4 × 10 μg) during weeks 7 to 9. Tissue samples were collected 24 and 48 h after the last dose of TPA. BrdUrd-positive LRCs were localized in similar numbers to the hair follicle bulge regions in control CD34KO and WT mice (Fig. 3*D*). When BrdUrd-labeled bulge cells are stimulated to proliferate, the labeled nuclei exhibit a speckled pattern consistent with cell division (46). In addition, the number of labeled nuclei within the hair follicle bulge decreases as stem cell progeny migrate upward out of the bulge into the infundibulum and downward to form the lower hair follicle (43, 44, 46). This dilution response can be visualized in WT hair follicle after both doses of TPA (Fig. 3*E*), where the number of labeled cells within the bulge is reduced as expected with transition into anagen growth (43, 44). In contrast, BrdUrd-labeled nuclei are still heavily stained and remain concentrated in the bulge region in CD34KO hair follicles, consistent with lack of activation and transition out of telogen (Fig. 3*E*). The skin of DMBA-initiated, TPA-promoted mice from the tumor studies described previously were examined 1 week after cessation of dosing. Anagen follicles were evident in all strains (data not shown), indicating that the hair follicles of CD34KO mice are capable of entering into active growth with continued TPA treatment. These data suggest that CD34 plays an important role in bulge cell activation in response to proliferative signals generated in the skin by TPA exposure and that the lack of bulge cell activation in the early stages of promotion contributes to the inability to form papillomas.

MTS24 Labeling in Basal Cells of TPA-Treated WT Epidermis

Recently, a population of hair follicle cells located between the mouse sebaceous gland and hair follicle bulge region has been shown to label with the MTS24 antibody, a cell surface marker that was originally described as a marker for thymic epithelial progenitor cells (47, 48). Although MTS24-positive cells do not express CD34 or keratin 15, and have relatively few LRCs, they nonetheless exhibit increased colony growth in clonogenic culture (29). However, it remains unknown whether this population is derived from bulge cells or represents an independent progenitor cell population. Because MTS24-positive hair follicle cells are potentially derived from CD34-positive bulge stem cells (29), we investigated whether MTS24 localization would be altered in the hair follicles of CD34KO mice. In addition, we were interested in the response of MTS24-positive hair follicle cells to TPA exposure in WT and CD34KO mice to determine if this population potentially contributed to the hair follicle phenotype described above (Fig. 3*B* and *C*). MTS24 was similarly localized in hair follicles of 7-week-old untreated WT and CD34KO mice (Fig. 4, *top*). Although levels of MTS24 reactivity increased in anagen hair follicles in TPA-treated mice (shown WT; Fig. 4, *bottom left*), this is consistent with observations in spontaneous anagen in adult mice (29) and is therefore not likely related to TPA exposure. Unexpectedly, MTS24 labeling was observed in the interfollicular epidermis of TPA-treated WT mice (Fig. 4, *bottom left* and *bottom middle*), whereas staining remained restricted to the hair follicles of CD34KO mice in spite of moderate TPA-induced hyperplasia (4 × 10 μg TPA at the 48-h time point shown for both strains; Fig. 4, *bottom right*). In WT mice, MTS24 staining in the interfollicular epidermis was most abundant at the high dose of TPA (4 × 10 μg) and at 48 h after the last dose, although staining was noted at both time points at both doses of TPA (data not shown). Staining was mostly restricted to basal cells within the interfollicular epidermis (Fig. 4, *bottom middle*), but suprabasal staining was noted in some instances as shown in Fig. 4 (*bottom left*). Because MTS24 has not been observed in the interfollicular epidermis of adult mice regardless of hair follicle stage (29), these findings show that MTS24 labeling in the hyperplastic epidermis is unique to TPA and suggests an association with MTS24-labeled cells emerging from the hair follicle into the interfollicular epidermis. Therefore, the differential staining pattern in TPA-treated WT and CD34KO skin may ultimately provide insight into the behavior of hair follicle progenitor cell response to TPA and the recruitment of initiated cells into the interfollicular epidermis during tumor promotion.

Discussion

We report here that the stem and progenitor cell marker CD34 is required for skin tumor development in mice. Our evidence suggests that the underlying mechanism governing the loss of tumor-forming capacity in CD34KO mice involves disruption in the normal response of the hair follicle stem and progenitor cell population to proliferative signals elicited by TPA exposure.

Several lines of evidence indicate that at least one population of carcinogen target cells resides in the hair follicle in the two-stage mouse model of skin carcinogenesis. Because tumors can arise from initiated skin even with promotion beginning after several hair cycle generations, it is reasonable to assume that these cells must not participate in the normal cell turnover to persist (9, 12, 49). Recent work has shown that carcinogen target cells form both in the interfollicular epidermis and in hair follicles, which is shown by a 50% reduction in papilloma development in mice in which the epidermis was removed after initiation (12). Based on this, we initially hypothesized that there would be a 50% reduction in skin tumor development in initiated/promoted CD34KO mice and that CD34 may have a functional role in bulge cell response to proliferative signals. We hypothesized that carcinogen target cells in the interfollicular epidermis would likely bypass CD34-mediated effects and retain the ability to form tumors.

In our initial studies, the complete lack of tumor development in CD34KO mice was unexpected. This suggested that CD34 was required for tumor development whether intrinsic to the keratinocyte in bulge cells or extrinsic in cellular components of the stromal compartment, including CD34-positive mast and endothelial cells. With regard to the latter, inflammatory cell composition, mast cell numbers, and angiogenesis (data not shown) are similar between strains following TPA treatment, suggesting that loss of CD34 outside of the epidermis is less likely to contribute to tumorigenesis. In addition, expression of other proteins [e.g., endoglycan on

endothelial cells (50) or CD43 on mast cells (20)] can act in a compensatory manner and preserve normal function, offering in part an explanation for the relatively normal physiology exhibited by CD34KO mice. Although our data do not indicate significant differences between the CD34KO and WT strains, we cannot rule out a contribution of nonepithelial components to tumor development.

The lack of tumor formation, particularly with regard to initiated cells within the interfollicular epidermis, led us to consider the possibility of a defect in DMBA-induced adduct formation, thus implicating perturbation in initiation as the critical component in the tumor phenotype. DNA adduct analysis tended to rule this out, however, because the CD34KO mice were clearly capable of metabolically activating DMBA into carcinogenic diol epoxides at the two different dose levels tested. It is interesting to note that, in the experiments where mice were initiated with 200 nmol DMBA, at the time WT mice began to give evidence of squamous exophytic foci (after 6–7 weeks of promotion), the skin of some CD34KO mice showed similar foci but these never developed into papillomas, suggesting that tumor-forming potential was present. Indeed, we found that increasing the initiating dose of DMBA to 400 nmol did result in papilloma formation in the CD34KO mice, albeit with a 7-week latency. The delay in papilloma formation combined with the virtually identical DNA adduct profile between strains showed that the CD34KO mice were essentially competent at initiation. Therefore, the tumor phenotype was most likely due to an effect on factors affecting promotion and outgrowth of initiated cells.

Several important studies have clearly shown that stem cell progeny migrate out of the bulge and form the lower hair follicle (4, 46, 51). Bulge cell progeny have also been shown to populate the basal layer of the interfollicular epidermis on wounding (5, 7, 46, 52). In addition, it has been shown the bulge cells transiently proliferate at anagen onset (44) and are stimulated to proliferate following TPA exposure (43, 44). With regard to papilloma formation, Binder et al. (53) provided evidence suggesting that, with TPA promotion, initiated cells from the hair follicle populate the infundibulum, proliferate and extend into the interfollicular epidermis, and eventually expand into papillomas. Our studies suggests that, in the absence of CD34, bulge cells are not activated appropriately in response to proliferative signals emerging either from hyperplastic epidermis or from inflammatory cells in the dermis following TPA exposure. This results in a delayed transition into anagen growth and altered migration of potential initiated cells into the proliferative environment of the TPA-treated interfollicular epidermis. Support for a critical role for bulge cell progeny in tumor development comes from the failure of signal transducers and activators of transcription 3 (STAT3) KO mice to develop tumors following a similar initiation/promotion regimen (54). Apoptosis of bulge cells lacking STAT3 expression following DMBA exposure at initiation most likely contributed to the failure to develop tumors (54), highlighting the importance of this population to papilloma formation in mice.

Our observations may also be supported by the evidence of MTS24 staining in the basal cells of the interfollicular epidermis of WT, but not CD34KO, mice following TPA treatment. MTS24-positive cells are normally restricted to the region between the sebaceous gland and the bulge region within the hair follicle (29); our data show that labeling in the interfollicular epidermis of TPA-treated WT mice is typically associated with labeling within the hair follicle. Although lineage studies are necessary to define this relationship, these data are suggestive that MTS24-labeled cells are emerging into the interfollicular epidermis from the hair follicle with TPA treatment rather than expression being induced in basal cells by TPA exposure. Therefore, lack of MTS24 staining in the interfollicular epidermis of TPA-treated CD34KO mice may be associated with failure of hair follicle cell migration into the interfollicular epidermis following TPA stimulation. It should be noted that hair follicles in CD34KO skin are capable of spontaneous anagen and normal hair growth. Based on this, we speculate that the biological role of CD34 may differ in the epithelial-mesenchymal signaling that occurs during normal follicular cycling versus that which is stimulated under wounding or other highly proliferative conditions. Although the underlying mechanism is unknown, CD34 may significantly affect the adhesive properties of bulge stem cells as well as in proliferation and differentiation based on the presence of functional protein kinase C phosphorylation sites (55). Key regulators of CD34 expression, including c-*myc* (56) and *TGFβ1* (57), may also position CD34 as a mediator of stem cell proliferation, migration, and cell fate decisions.

In summary, our data suggest that CD34 may be a participant in hair follicle bulge cell activation and provide evidence that bulge cell progeny are required for skin tumor development in mice. These findings highlight the potential contribution of stem cells to skin carcinogenesis and offer an opportunity for gaining insight into the earliest stages of neoplastic development.

Acknowledgments

Received 8/23/2006; revised 12/21/2006; accepted 2/20/2007.

Grant support: NIH grant CA97957 (R.J. Morris and G. Cotsarelis), Dutch Cancer Society grant RUL 2002-2737 (J.G.W. Nijhof), and Intramural Research Program of the NIH and National Institute of Environmental Health Sciences (NIEHS).

The costs of publication of this article were defrayed in part by the payment of page charges. This article must therefore be hereby marked *advertisement* in accordance with 18 U.S.C. Section 1734 solely to indicate this fact.

We thank Drs. Robert Langenbach, Colin Chigell (NIEHS), Stephen Nesnow, and Douglas Wolf (United States Environmental Protection Agency) for their critical review of this manuscript; Julie Foley (NIEHS and head of the NIEHS Special Techniques Group), Theleria Hackett and the histology staff at Integrated Laboratory Systems, Inc., Beth Mahler (PAI), and the NIEHS Arts and Photography Staff; Dr. Robert Boyd (Monash University, Melbourne, Victoria, Australia) for providing the MTS2 antibody; and Miriam Sander (Page One Editorial Services, Durham, NC) for her expert help in preparing this manuscript.

References

1. Cotsarelis G, Sun TT, Lavker RM. Label-retaining cells reside in the bulge area of pilosebaceous unit: implications for follicular stem cells, hair cycle, and skin carcinogenesis. Cell 1990;61:1329–37.
2. Fuchs E, Tumbar T, Guasch G. Socializing with the neighbors: stem cells and their niche. Cell 2004;116:769–78.
3. Lavker RM, Sun TT. Epidermal stem cells: properties, markers, and location. Proc Natl Acad Sci U S A 2000;97:13473–5.
4. Morris RJ, Liu Y, Marles L, et al. Capturing and profiling adult hair follicle stem cells. Nat Biotechnol 2004;22:411–7.
5. Claudinot S, Nicolas M, Oshima H, Rochat A, Barrandon Y. Long-term renewal of hair follicles from clonogenic multipotent stem cells. Proc Natl Acad Sci U S A 2005;102:14677–82.
6. Ito M, Liu Y, Yang Z, et al. Stem cells in the hair follicle bulge contribute to wound repair but not to homeostasis of the epidermis. Nat Med 2005;11:1351–4.
7. Levy V, Lindon C, Harfe BD, Morgan BA. Distinct stem cell populations regenerate the follicle and interfollicular epidermis. Dev Cell 2005;9:855–61.
8. Morris RJ. Keratinocyte stem cells: targets for cutaneous carcinogens. J Clin Invest 2000;106:3–8.
9. Owens DM, Watt FM. Contribution of stem cells and differentiated cells to epidermal tumours. Nat Rev Cancer 2003;3:444–51.
10. DiGiovanni J. Multistage carcinogenesis in mouse skin. Pharmacol Ther 1992;54:63–128.
11. Yuspa SH. The pathogenesis of squamous cell cancer: lessons learned from studies of skin carcinogenesis—thirty-third G. H. A. Clowes Memorial Award Lecture. Cancer Res 1994;54:1178–89.
12. Morris RJ, Tryson KA, Wu KQ. Evidence that the epidermal targets of carcinogen action are found in the interfollicular epidermis of infundibulum as well as in the hair follicles. Cancer Res 2000;60:226–9.
13. Jones PH, Watt FM. Separation of human epidermal

stem cells from transit amplifying cells on the basis of differences in integrin function and expression. Cell 1993;73:713–24.
14. Tani H, Morris RJ, Kaur P. Enrichment for murine keratinocyte stem cells based on cell surface phenotype. Proc Natl Acad Sci U S A 2000;97:10960–5.
15. Trempus CS, Morris RJ, Bortner CD, et al. Enrichment for living murine keratinocytes from the hair follicle bulge with the cell surface marker CD34. J Invest Dermatol 2003;120:501–11.
16. Li L, Mignone J, Yang M, et al. Nestin expression in hair follicle sheath progenitor cells. Proc Natl Acad Sci U S A 2003;100:9958–61.
17. Tumbar T, Guasch G, Greco V, et al. Defining the epithelial stem cell niche in skin. Science 2004; 303:359–63.
18. Blanpain C, Lowry WE, Geoghegan A, Polak L, Fuchs E. Self-renewal, multipotency, and the existence of two cell populations within an epithelial stem cell niche. Cell 2004;118:635–48.
19. Krause DS, Ito T, Fackler MJ, et al. Characterization of murine CD34, a marker for hematopoietic progenitor and stem cells. Blood 1994;84:691–701.
20. Drew E, Merkens H, Chelliah S, Doyonnas R, McNagny KM. CD34 is a specific marker of mature murine mast cells. Exp Hematol 2002;30:1211–8.
21. Baumheter S, Singer MS, Henzel W, et al. Binding of L-selectin to the vascular sialomucin CD34. Science 1993;262:436–8.
22. Poblet E, Jimenez-Acosta F, Rocamora A. QBEND/10 (anti-CD34 antibody) in external root sheath cells and follicular tumors. J Cutan Pathol 1994;21:224–8.
23. Cotsarelis G. Epithelial stem cells: a folliculocentric view. J Invest Dermatol 2006;126:1459–68.
24. Ohyama M, Terunuma A, Tock CL, et al. Characterization and isolation of stem cell-enriched human hair follicle bulge cells. J Clin Invest 2006;116:249–60.
25. Rosen SD. Ligands for L-selectin: homing, inflammation, and beyond. Annu Rev Immunol 2004;22:129–56.
26. Drew E, Merzaban JS, Seo W, Ziltener HJ, McNagny KM. CD34 and CD43 inhibit mast cell adhesion and are required for optimal mast cell reconstitution. Immunity 2005;22:43–57.
27. Felschow DM, McVeigh ML, Hoehn GT, Civin CI, Fackler MJ. The adapter protein CrkL associates with CD34. Blood 2001;97:3768–75.
28. Suzuki A, Andrew DP, Gonzalo JA, et al. CD34-deficient mice have reduced eosinophil accumulation after allergen exposure and show a novel crossreactive 90-kD protein. Blood 1996;87:3550–62.
29. Nijhof JG, Braun KM, Giangreco A, et al. The cell-surface marker MTS24 identifies a novel population of follicular keratinocytes with characteristics of progenitor cells. Development 2006;133:3027–37.
30. Lee H, Harvey RG. Synthesis of the active diol epoxide metabolites of the potent carcinogenic hydrocarbon 7,12-dimethylbenz[a]anthrene. J Org Chem 1986; 51:3502–7.
31. Sharma AK, Amin S, Kumar S. An abbreviated synthesis of 7,12-dimethylbenz[*a*]anthracene and benzo[*c*]chrysene metabolites using the Suzuki reaction. Poly Arom Com 2002;22:277–88.
32. Wu WY, Morris RJ. Method for the harvest and assay of *in vitro* clonogenic keratinocytes stem cells from mice. Methods Mol Biol 2005;289:79–86.
33. King LC, Adams L, Allison J, et al. A quantitative comparison of dibenzo[*a,l*]pyrene-DNA adduct formation by recombinant human cytochrome P450 microsomes. Mol Carcinog 1999;26:74–82.
34. Lau HH, Baird WM. Detection and identification of benzo[a]pyrene-DNA adducts by [^{35}S]phosphorothioate labeling and HPLC. Carcinogenesis 1991;12:885–93.
35. King LC, George M, Gallagher JE, Lewtas J. Separation of ^{32}P-postlabeled DNA adducts of polycyclic aromatic hydrocarbons and nitrated polycyclic aromatic hydrocarbons by HPLC. Chem Res Toxicol 1994;7:503–10.
36. King LC, Kohan MJ, Brooks L, et al. An evaluation of the mutagenicity, metabolism, and DNA adduct formation of 5-nitrobenzo[*b*]naphtho[2,1-*d*]thiophene. Chem Res Toxicol 2001;14:661–71.
37. Weyand EH, Rice JE, LaVoie EJ. ^{32}P-postlabeling analysis of DNA adducts from non-alternant PAH using thin-layer and high performance liquid chromatography. Cancer Lett 1987;37:257–66.
38. Reiners JJ, Jr., Singh KP. Susceptibility of 129/SvEv mice in two-stage carcinogenesis protocols to 12-*O*-tetradecanoylphorbol-13-acetate promotion. Carcinogenesis 1997;18:593–7.
39. Lundberg P, Welander P, Openshaw H, et al. A locus on mouse chromosome 6 that determines resistance to herpes simplex virus also influences reactivation, while an unlinked locus augments resistance of female mice. J Virol 2003;77:11661–73.
40. Lyle S, Christofidou-Solomidou M, Liu Y, Elder DE, Albelda S, Cotsarelis G. Human hair follicle bulge cells are biochemically distinct and possess an epithelial stem cell phenotype. J Investig Dermatol Symp Proc 1999;4:296–301.
41. Ito M, Kizawa K. Expression of calcium-binding S100 proteins A4 and A6 in regions of the epithelial sac associated with the onset of hair follicle regeneration. J Invest Dermatol 2001;116:956–63.
42. Balmain A, Ramsden M, Bowden GT, Smith J. Activation of the mouse cellular Harvey-ras gene in chemically induced benign skin papillomas. Nature 1984;307:658–60.
43. Braun KM, Niemann C, Jensen UB, Sundberg JP, Silva-Vargas V, Watt FM. Manipulation of stem cell proliferation and lineage commitment: visualisation of label-retaining cells in wholemounts of mouse epidermis. Development 2003;130:5241–55.
44. Wilson C, Cotsarelis G, Wei ZG, et al. Cells within the bulge region of mouse hair follicle transiently proliferate during early anagen: heterogeneity and functional differences of various hair cycles. Differentiation 1994; 55:127–36.
45. Bickenbach JR. Identification and behavior of label-retaining cells in oral mucosa and skin. J Dent Res 1981; 60 Spec No C:1611–20.
46. Taylor G, Lehrer MS, Jensen PJ, Sun TT, Lavker RM. Involvement of follicular stem cells in forming not only the follicle but also the epidermis. Cell 2000;102:451–61.
47. Bennett AR, Farley A, Blair NF, Gordon J, Sharp L, Blackburn CC. Identification and characterization of thymic epithelial progenitor cells. Immunity 2002; 16:803–14.
48. Gill J, Malin M, Hollander GA, Boyd R. Generation of a complete thymic microenvironment by MTS24(+) thymic epithelial cells. Nat Immunol 2002;3:635–42.
49. Morris RJ, Tacker KC, Fischer SM, Slaga TJ. Quantitation of primary *in vitro* clonogenic keratinocytes from normal adult murine epidermis, following initiation, and during promotion of epidermal tumors. Cancer Res 1988;48:6285–90.
50. Sassetti C, Van Zante A, Rosen SD. Identification of endoglycan, a member of the CD34/podocalyxin family of sialomucins. J Biol Chem 2000;275:9001–10.
51. Oshima H, Rochat A, Kedzia C, Kobayashi K, Barrandon Y. Morphogenesis and renewal of hair follicles from adult multipotent stem cells. Cell 2001; 104:233–45.
52. Ito M, Kizawa K, Hamada K, Cotsarelis G. Hair follicle stem cells in the lower bulge form the secondary germ, a biochemically distinct but functionally equivalent progenitor cell population, at the termination of catagen. Differentiation 2004;72:548–57.
53. Binder RL, Johnson GR, Gallagher PM, Stockman SL, Sundberg JP, Conti CJ. Squamous cell hyperplastic foci: precursors of cutaneous papillomas induced in SENCAR mice by a two-stage carcinogenesis regimen. Cancer Res 1998;58:4314–23.
54. Chan KS, Sano S, Kiguchi K, et al. Disruption of Stat3 reveals a critical role in both the initiation and the promotion stages of epithelial carcinogenesis. J Clin Invest 2004;114:720–8.
55. Lanza F, Healy L, Sutherland DR. Structural and functional features of the CD34 antigen: an update. J Biol Regul Homeost Agents 2001;15:1–13.
56. Radomska HS, Satterthwaite AB, Burn TC, Oliff IA, Huettner CS, Tenen DG. Multiple control elements are required for expression of the human CD34 gene. Gene 1998;222:305–18.
57. Marone M, Scambia G, Bonanno G, et al. Transforming growth factor-β1 transcriptionally activates CD34 and prevents induced differentiation of TF-1 cells in the absence of any cell-cycle effects. Leukemia 2002; 16:94–105.

CD34 Expression by Hair Follicle Stem Cells Is Required for Skin Tumor Development in Mice

Carol S. Trempus, Rebecca J. Morris, Matthew Ehinger, et al.

Cancer Res 2007;67:4173-4181.